Fermilab-Pub-16-190-T

Multi-step production of a diphoton resonance

Bogdan A. Dobrescu, Patrick J. Fox and John Kearney

Theoretical Physics Department, Fermilab, Batavia, IL 60510, USA

May 27, 2016

arXiv:1605.08772v1 [hep-ph] 27 May 2016

Abstract

Assuming that the mass peak at 750 GeV reported by the ATLAS and CMS Collaborations is due to a spin-0 particle that decays into two photons, we present two weakly-coupled renormalizable models that lead to different production mechanisms. In one model, a scalar particle produced through gluon fusion decays into the diphoton particle and a light, long-lived pseudoscalar. In another model, a Z' boson produced from the annihilation of a strange-antistrange quark pair undergoes a cascade decay that leads to the diphoton particle and two sterile neutrinos. We show that various kinematic distributions may differentiate these models from the canonical model where the diphoton particle is directly produced in gluon fusion.

Contents

1 Introduction **2**

2 A 2-step scalar model **3**

2.1 Scalar interactions 4

2.2 Branching fractions of A 6

2.3 LHC signal rate in the 2-step model 8

3 A strange-production model **12**

3.1 New fields and symmetries 12

3.2 Production and decay 16

4 Kinematic distributions **19**

5 Conclusions **23**

Operated by Fermi Research Alliance, LLC under Contract No. De-AC02-07CH11359 with the United States Department of Energy

1 Introduction

In Run 2 of the LHC, started in 2015, the proton-proton collisions at a center-of mass energy of 13 TeV open a large new window towards the laws of nature at the shortest distances directly accessible so far.

In March 2016, the ATLAS and CMS Collaborations have presented additional information [1, 2] related to the excess diphoton events first reported in December 2015 [3, 4]. The CMS Collaboration has refined the analysis of the 2.7 fb^{-1} of 13 TeV LHC data, and included an additional 0.6 fb^{-1} of data obtained with no magnetic field. This has increased the deviation from the SM to 2.9σ at a diphoton invariant mass of 750 GeV. When combined with the 8 TeV data [5] assuming a gluon-gluon initial state, the local significance of the CMS excess is 3.4σ [2].

More importantly, the ATLAS Collaboration has released several kinematic distributions associated with the signal region of the diphoton invariant mass distribution [1]. This allows discrimination between various theoretical models that could accommodate the diphoton peak. Furthermore, the new ATLAS analysis of the 8 TeV data, optimized for a spin-0 $\gamma\gamma$ resonance, shows an independent 1.9σ excess at 750 GeV, which is compatible (for production via gluon fusion and with 6% width-to-mass ratio) with the 3.9σ peak in the 13 TeV data reported by ATLAS.

Although these peaks may be due to unlikely fluctuations of the Standard Model (SM) backgrounds, it is useful to analyze possible explanations in terms of new particles. Many theoretical studies have been devoted to a canonical interpretation of these peaks under the assumption of a particle produced from a gluon-gluon initial state that decays into directly two photons (for reviews, see [6, 7], for earlier work see, *e.g.*, [8]).

Here we present a couple of renormalizable models in which the diphoton resonance arises from cascade decays of some slightly heavier particles. In the first model, a scalar particle produced in gluon fusion decays into two pseudoscalars, one of which (A) is the diphoton resonance and the other (A') is very light and quasi-stable (we refer to this as a 2-step model). In the second model, a Z' boson couples to the right-handed s and b quarks as well as to two new fermions, N and ν_s, which are singlets under the SM gauge group. One of the Z' decay modes is into $\bar{\nu}_s N$, with a subsequent decay of N into ν_s and the diphoton resonance (we refer to this as a 3-step model). We explore whether the kinematic distributions can eventually differentiate between these models.

Two-step production topologies[1] were previously considered in [12, 13] in the context of simplified models, before the public release of the ATLAS kinematic distributions. A more complete 2-step model is discussed in [14] in the context of the NMSSM; the presence of a couple of b jets in each diphoton event appears now to be in conflict with the data.

Our renormalizable 2-step model naturally accommodates the small mass splitting between the scalar (φ) produced in gluon fusion and the pseudoscalar A that decays into photons by embedding them into the same complex scalar field. The pseudoscalar A' that escapes the detector is naturally very light because it is the pseudo-Nambu Goldstone boson associated with a $U(1)$ symmetry. Thus, the fit to the ATLAS kinematic distributions does not require tuning. In addition, having a renormalizable model allows us to establish that the diphoton rate can be as large as indicated by the data.

The 3-step model is more peculiar, because the s-channel resonance is a spin-1 particle (an alternative model is discussed in [11]) and the initial state is mostly a strange-antistrange pair. Even though the small mass splittings are put in by hand in this model, it is useful to have a renormalizable model that does not involve gluon fusion (and thus leads to less initial state radiation) and yet is consistent with a large cross section increase from $\sqrt{s} = 8$ TeV to 13 TeV.

In Section 2 we present the 2-step scalar model, compute the diphoton rate, and discuss other phenomenological implications. In Section 3 we construct and analyze the 3-step Z' model. The kinematic distributions predicted in these models, as well as in the canonical "1-step" model, are compared with the ATLAS data in Section 4. Our conclusions are presented in Section 5.

2 A 2-step scalar model

In this section we present a simple model in which the spin-0 particle produced in gluon fusion is different than the spin-0 particle that decays into a photon pair. The model consists of two complex scalar fields, ϕ and ϕ', which are SM singlets, a real scalar field Θ^a that is a color-octet ($a = 1, ..., 8$), and a vectorlike lepton ψ of electric charge one.

[1] Our model has little in common with the "2-step decay" studied in [9]. Also, the fact that A and A' are different particles (with a large mass splitting) distinguishes our 2-step model from the model where two 750 GeV particles are simultaneously produced [10, 11], which no longer seems viable in light of the recent ATLAS $\not{E}_T$ distribution.

The SM-singlet scalars are formed of the following real scalar fields:

$$\phi = \langle\phi\rangle + \frac{1}{\sqrt{2}}\,(\varphi + iA) \quad ,$$

$$\phi' = \langle\phi'\rangle + \frac{1}{\sqrt{2}}\,(\varphi' + iA') \quad , \tag{2.1}$$

We consider the case where the VEVs satisfy $\langle\phi'\rangle \gg \langle\phi\rangle > 0$. We will neglect the ϕ VEV for now, and we will check later that this is a fair approximation. The masses of the two CP-even scalars φ and φ', M_φ and $M_{\varphi'}$, satisfy $M_\varphi < M_{\varphi'}$; φ' will not be important in what follows. The masses of the two CP-odd scalars A and A' satisfy $M_A \approx 750$ GeV, $M_{A'} \ll M_A$ and $M_\varphi > M_A + M_{A'}$.

The interactions of these spin-0 particles will be selected such that the cascade decay $\varphi \to A'A \to A'\gamma\gamma$ has a large branching fraction, and A' does not decay inside the detector.

2.1 Scalar interactions

We assume that ϕ interacts with the color-octet scalar, Θ^a, via the following CP-conserving term in the Lagrangian:

$$-\frac{\kappa}{2}\,\phi'\phi\,\Theta^a\Theta^a + \text{H.c.} \supset -\frac{\kappa\langle\phi'\rangle}{\sqrt{2}}\,\varphi\,\Theta^a\Theta^a \quad , \tag{2.2}$$

where κ is a real dimensionless parameter. This coupling leads at one loop to $gg \to \varphi$ production at the LHC [15, 16]. Other terms in the potential that involve Θ^a are given by

$$V(\Theta) = \frac{1}{2}\left(M_\theta^2 + \kappa_1|\phi|^2 + \kappa_2|\phi'|^2\right)\Theta^a\Theta^a + \frac{\lambda_\Theta}{8}\left(\Theta^a\Theta^a\right)^2 + \mu_\Theta\, d_{abc}\Theta^a\Theta^b\Theta^c \quad . \tag{2.3}$$

Here $\lambda_\Theta > 0$ is a dimensionless parameter relevant in Section 2.3, and μ_Θ is a trilinear coupling that allows the decay $\Theta \to gg$ at one loop [17]. The first term in $V(\Theta)$ leads to a squared-mass for the color-octet particle, $M_\Theta^2 \simeq M_\theta^2 + \kappa_2\langle\phi'\rangle^2$, which we take to be positive.

The ϕ and ϕ' fields have a dimension-4 coupling in the potential,

$$V_\lambda = \frac{\lambda}{4}\,(\phi\,\phi')^2 + \text{H.c.} \quad , \tag{2.4}$$

which includes the following interaction of φ with the CP-odd scalars in the Lagrangian:

$$\frac{\lambda\langle\phi'\rangle}{\sqrt{2}}\,\varphi\,AA' \quad . \tag{2.5}$$

As a result, the φ scalar decays into AA' with a width

$$\Gamma(\varphi \to AA') = \frac{\lambda^2 \langle\phi'\rangle^2}{32\pi M_\varphi} \left[\left(1+\frac{M_A}{M_\varphi}\right)^2 - \frac{M_{A'}^2}{M_\varphi^2}\right]^{1/2} \left[\left(1-\frac{M_A}{M_\varphi}\right)^2 - \frac{M_{A'}^2}{M_\varphi^2}\right]^{1/2} \quad . \tag{2.6}$$

Even though this width is phase-space suppressed, the $\varphi \to AA'$ branching fraction is large because the only other significant decay mode of φ, into two gluons, is loop-suppressed; a quantitative assessment is postponed until Section 2.3. The primary ingredient necessary for explaining the diphoton peak is thus in place: the "2-step production" $gg \to \varphi \to AA'$. The subsequent $A \to \gamma\gamma$ decay, discussed in Section 2.2, then gives rise to a diphoton signal at the LHC (see the diagram in Figure 1).

The scalar interactions introduced so far, and below, exhibit a (spontaneously-broken) global $U(1)$ symmetry under which ϕ and ϕ' rotate oppositely. The full scalar potential allowed by this symmetry is

$$V(\phi,\phi') = M_0^2|\phi|^2 - M_0'^2|\phi'|^2 - (b^2\phi\phi' + \text{H.c.}) + \frac{\lambda_1}{2}|\phi|^4 + \frac{\lambda_2}{2}|\phi'|^4 + \lambda_3|\phi\phi'|^2 + V_\lambda \quad . \tag{2.7}$$

We assume that all parameters are real and positive and thus any VEVs are also positive. In addition we take $b^2 \ll M_0^2$ so that $\langle\phi'\rangle \approx M_0'/\sqrt{\lambda_2} \gg \langle\phi\rangle$. Note that the VEV of ϕ is induced by the b^2 term,

$$\langle\phi\rangle \approx \frac{b^2\langle\phi'\rangle}{M_0^2 + (\lambda_3+\lambda/2)\langle\phi'\rangle^2} \quad . \tag{2.8}$$

In the $b/M_0 \to 0$ limit, the Nambu-Goldstone boson arising from the spontaneously broken $U(1)$ is the A' component of ϕ'. That limit, however, is unstable because the coupling to Θ in Eq. (2.2) induces a 1-loop contribution to b^2. For $b^2 \neq 0$, the Nambu-Goldstone boson is a linear combination of A' and A. In practice it is sufficient to have $b/M_0 \lesssim 0.3$, as the corrections to the φ branching fractions and to the $M_\varphi - M_A$ mass splitting are only of order b^4/M_0^4. We will neglect these corrections, so we will keep the A' notation for the Nambu-Goldstone boson.

With the Lagrangian introduced so far, A' remains strictly massless. A small A' mass can be easily induced by including an explicit breaking of the global $U(1)$, for example a $M_{A'}^2\phi'^2$ term with $M_{A'} \ll |M_0'|$. As discussed in Section 2.3, values of $M_{A'}$ as low as 6 MeV (and perhaps lower) are phenomenologically viable.

The quartic interaction V_λ also leads to a mass splitting of φ and A:

$$M_{\varphi,A}^2 = M_0^2 + \left(\lambda_3 \pm \frac{\lambda}{2}\right)\langle\phi'\rangle^2 \quad , \tag{2.9}$$

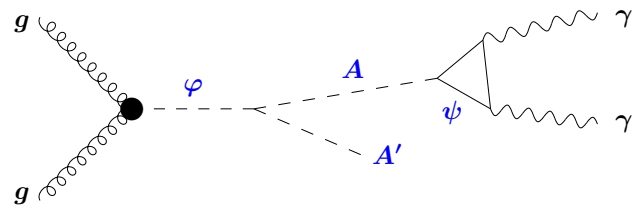

Figure 1: Diagram for A production at the LHC in the 2-step model, where A is a CP-odd scalar of mass at 750 GeV. A' is a light pseudoscalar that escapes the detector. The black disk represents the sum over loop contributions from the color-octet scalar Θ.

so that the mass-squared difference is

$$M_\varphi^2 - M_A^2 = \lambda \langle \phi' \rangle^2 \quad . \tag{2.10}$$

The V_λ term can be induced at 1-loop from the coupling to Θ, thus in the absence of fine tuning one would expect that $\lambda \gtrsim \kappa^2/(8\pi^2)$. At the same time, the diphoton kinematic distributions [1] require $M_\varphi - M_A \lesssim O(50)$ GeV, so that λ must be smaller than about $0.12 M_\varphi^2/\langle \phi' \rangle^2$.

2.2 Branching fractions of A

To generate the diphoton signal, we introduce interactions allowing the decay $A \to \gamma\gamma$. This can be accomplished by coupling the scalars ϕ and ϕ' to the vectorlike lepton ψ,

$$- y_\psi \, \phi \, \bar{\psi}_L \psi_R - y'_\psi \, \phi' \, \bar{\psi}_R \psi_L + \text{H.c.} \quad , \tag{2.11}$$

where the Yukawa couplings are $y_\psi, y'_\psi > 0$. We assign global $U(1)$ charges to ψ_L and ψ_R such that the above terms are $U(1)$ invariant. As a result, a mass term for ψ can be generated only by the $U(1)$ breaking VEVs. Thus, the vectorlike lepton has a mass

$$m_\psi \simeq y'_\psi \langle \phi' \rangle \quad . \tag{2.12}$$

The Yukawa interactions (2.11) contribute at one loop to the b^2 term in $V(\phi, \phi')$. Hence, the values of the VEVs shift slightly. We neglect the effects of the ψ loops, as they are not larger than those of the Θ loops discussed in Section 2.1. As before, A' remains a massless Nambu-Goldstone boson unless we choose to include explicit $U(1)$ breaking terms.

The first term in Eq. (2.11) includes the following interaction:

$$- y_\psi \, i A \bar{\psi} \gamma_5 \psi \quad . \tag{2.13}$$

For $m_\psi > M_A/2$, the vectorlike lepton can be integrated out leading to a dimension-5 interaction of the CP-odd scalar A with two SM gauge bosons. If ψ is an $SU(2)_W$ singlet of hypercharge $+1$, the dimension-5 interaction is given by

$$\frac{\alpha\, y_\psi}{8\sqrt{2}\pi\, m_\psi \cos^2\theta_w}\, A\, B^{\mu\nu}\widetilde{B}_{\mu\nu} \quad . \tag{2.14}$$

The resulting width for the A decay into photons is given by

$$\Gamma(A \to \gamma\gamma) = \frac{\alpha^2\, y_\psi^2\, M_A^3}{128\pi^3\, m_\psi^2} \quad , \tag{2.15}$$

with the electromagnetic coupling constant α evaluated at a scale of order M_A. Besides couplings to photons, the operator (2.14) includes A interactions with $Z\gamma$ and ZZ, which give the following decay widths:

$$\begin{aligned} \Gamma(A \to Z\gamma) &= 2\tan^2\theta_w\, \Gamma(A \to \gamma\gamma) \quad , \\ \Gamma(A \to ZZ) &= \tan^4\theta_w\, \Gamma(A \to \gamma\gamma) \quad . \end{aligned} \tag{2.16}$$

Here θ_w is the electroweak mixing angle at the M_φ scale, so that $\tan^2\theta_w \approx 0.30$.

The quartic coupling of ϕ to Θ and ϕ' shown in Eq. (2.2) includes a

$$-\frac{\kappa}{2} A A'\, \Theta^a \Theta^a \tag{2.17}$$

interaction. Consequently, the A particle does not decay into gluons but it has a 1-loop, 3-body decay into $A'gg$:

$$\Gamma_1(A \to A'gg) \simeq \frac{\alpha_s^2\, \kappa^2\, M_A^5}{6\,(8\pi)^5 M_\Theta^4} \quad . \tag{2.18}$$

There is an additional contribution to the $A \to A'gg$ amplitude from an off-shell φ, which interferes with the one due to Eq. (2.17). However, this is a subdominant contribution when $M_\varphi - M_A \ll M_A$, and it can be safely neglected here. We expect that higher-order QCD corrections enhance $\Gamma(A \to A'gg)$ by a factor of order 2. Let us compute the widths for some benchmark point in the parameter space:

$$\begin{aligned} &\lambda = 0.1 \ \ , \ \ \langle\phi'\rangle = 680 \text{ GeV} \ \Rightarrow \ M_\varphi = 780 \text{ GeV} \quad , \\ &M_\Theta = 800 \text{ GeV} \ \ , \ \ \kappa = y_\psi = \lambda_\Theta = 1 \quad , \\ &y'_\psi = 1 \ \Rightarrow \ m_\psi = 680 \text{ GeV} \quad . \end{aligned} \tag{2.19}$$

The result $\Gamma(A \to A'gg) \approx 0.2$ keV is two orders of magnitude smaller than $\Gamma(A \to \gamma\gamma) \approx$ 14 keV. The branching fractions of A into $\gamma\gamma$, $Z\gamma$ and ZZ are thus 58.8%, 35.3% and 5.3%, respectively.

2.3 LHC signal rate in the 2-step model

For a Θ^a mass $M_\Theta > M_\varphi/2$, the coupling (2.2) induces an interaction of φ with gluons approximately given by the dimension-5 operator

$$\frac{\alpha_s \kappa \langle \phi' \rangle \, \mathcal{C}_\Theta \mathcal{C}_{\rm loop}}{16\sqrt{2}\pi M_\Theta^2} \, \varphi \, G^{\mu\nu\, a} \, G^{\, a}_{\mu\nu} \quad , \tag{2.20}$$

where $\mathcal{C}_\Theta$ is a coefficient that includes the deviations from the small $M_\varphi^2/(2M_\Theta)^2$ limit (the full expression without taking the large M_Θ limit can be extracted from [16]):

$$\mathcal{C}_\Theta = 1 + \frac{2M_\varphi^2}{15M_\Theta^2} + \frac{3M_\varphi^4}{140M_\Theta^4} + O\left(M_\varphi^6/(2M_\Theta)^6\right) \quad . \tag{2.21}$$

The coefficient $\mathcal{C}_{\rm loop}$ includes higher-order loop corrections:

$$\mathcal{C}_{\rm loop} \simeq 1 + \frac{33\alpha_s}{4\pi} + \frac{5\lambda_\Theta}{16\pi^2} \quad . \tag{2.22}$$

The first term here arises from integrating Θ^a out at one loop, while the next two terms arise at two loops and have been computed in [15]. The term proportional to λ_Θ involves one insertion of the quartic Θ coupling, see Eq. (2.3). We assumed $\mu_\Theta \ll M_\Theta$, so that the 2-loop contributions with trilinear Θ couplings are negligible.

The dimension-5 operator (2.20), which is responsible for φ production, also leads to the decays of φ into gluons and, at higher-orders in the QCD coupling, into quark pairs. These decays have a width given at the next-to-leading order by

$$\Gamma(\varphi \to gg, 3g, gq\bar{q}) \simeq \alpha_s^2(\mu_{\rm decay}) \, \frac{\kappa^2 \langle \phi' \rangle^2 M_\varphi^3}{256\pi^3 \, M_\Theta^4} \, \mathcal{C}_\Theta^2 \, \mathcal{C}_{\rm loop}^2 \times \left[1 + \frac{\alpha_s}{\pi} \left(\frac{73}{4} - \frac{7N_f}{6} - \frac{33 - 2N_f}{3} \ln \frac{M_\varphi}{\mu_{\rm decay}} \right) \right] \quad . \tag{2.23}$$

The next-to-leading order corrections [18] shown here depend on the number N_f of quark flavors lighter than $M_\varphi/2$. As the $gt\bar{t}$ final state is phase-space suppressed, the effective value of N_f is between 5 and 6. These corrections also depend on a renormalization scale, which is taken to be $\mu_{\rm decay} = M_\varphi$ in order to minimize higher-order corrections to the decay width [19]. The QCD coupling constant at the scale $M_\varphi = 780$ GeV is $\alpha_s(M_\varphi) \approx 0.092$ [20].

Besides the unavoidable decay into jets, there are a few other more model-dependent decay modes. Notably, the ϕ and ϕ' fields can couple to the SM Higgs doublet, H, via

$|\phi|^2 H^\dagger H$, $|\phi'|^2 H^\dagger H$, and $\phi\phi' H^\dagger H$ terms. The latter, in particular, must have a suppressed coefficient (below $\sim 3\times 10^{-2}$) to avoid a large mixing of φ with the SM Higgs boson h^0. Otherwise, the dominant decay mode of φ would be into top pairs, and the branching fraction $B(\varphi \to AA')$ would be too small. We ignore the $\varphi - h^0$ mixing in what follows.

In addition, the small but nonzero $\langle\phi\rangle$ VEV discussed in Section 2.1 leads to the $\varphi \to A'A'$ decay. The width for this decay is not phase-space suppressed, but it is proportional to $(\langle\phi\rangle/\langle\phi'\rangle)^2 < 10^{-2}$, and it can be neglected compared to the $\varphi \to A'A$ width. Another subdominant decay of φ is into $\gamma\gamma$, due to a ψ loop; its branching fraction, of order 0.1%, is too small to be phenomenologically relevant.

Comparing the main φ decay widths given in Eqs. (2.6) and (2.23), we find that the branching fraction for $\varphi \to AA'$ is sizable for a large range of parameters. For example, the benchmark point (2.19) implies $B(\varphi \to AA') \approx 73\%$ and a total width for φ given by $\Gamma_\varphi \approx 8\times 10^{-6} M_\varphi$.

The dimension-5 operator (2.20) also leads to s-channel production of φ at the LHC. In that case, the renormalization scale that minimizes the higher-order corrections is approximately $M_\varphi/2$. Including the interaction (2.20) in FeynRules [21] with a coefficient that depends on the QCD coupling constant at the $M_\varphi/2$ scale, $\alpha_s(390\text{ GeV}) \approx 0.097$, we have generated the model files for MadGraph [22] and obtained the leading-order cross section for inclusive φ production at the 13 TeV LHC:

$$\sigma_{\rm LO}(pp \to \varphi X) \approx 6.8\text{ fb}\,\left(\frac{\langle\phi'\rangle}{680\text{ GeV}}\right)^2 \kappa^2 \tag{2.24}$$

for $M_\varphi = 780$ GeV, $M_\Theta = 800$ GeV (and, less importantly, $\lambda_\Theta = 1$). Recall that Eq. (2.10) implies $\langle\phi'\rangle = 680$ GeV for $\lambda = 0.1$.

Higher-order corrections to φ production are large; we break them down as follows:

1) The next-to-leading order QCD corrections, using the dimension-5 interaction (2.20), which include 1-loop corrections as well as a real emission from the initial state partons. We have computed those using the MCFM code [23], and obtained a multiplicative K factor given by $K_{\rm NLO} = 1.88$.

2) The NNLO and N^{3}LO QCD corrections, again in the large M_Θ limit. These have been computed in the case of Higgs production [24], and amount to an additional 30% increase. In the case of our φ production, we expect that these corrections are smaller by a factor of roughly $\alpha_s(M_\varphi/2)/\alpha_s(M_h/2) \approx 0.8$, so that the total multiplicative factor becomes $K_{\rm N^3LO} \sim 1.24 K_{\rm NLO} \approx 2.3$. This estimate is consistent with the recent result of Ref. [25]

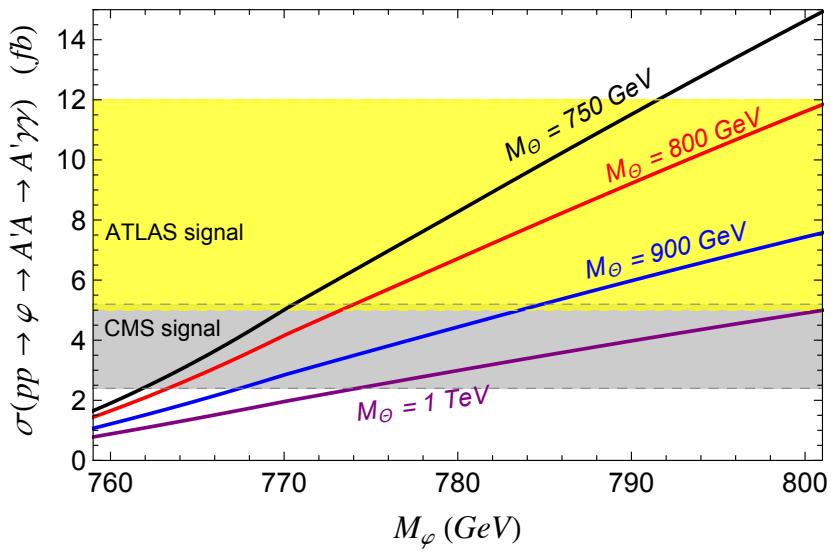

Figure 2: Diphoton signal cross section at the 13 TeV LHC in the 2-step model, as a function of the φ mass, for four different masses of the color-octet scalar Θ responsible for gluon fusion. The parameters used here are $\lambda = 0.1$, $\kappa = \lambda_\Theta = y'_\psi = 1$ and $M_{A'} = 0$. The gray and yellow shaded regions represent the 1σ bands of the CMS [2] and ATLAS (estimated in [26]) signal cross sections, respectively.

($K_{\mathrm{N^3LO}} \approx 2.3$ for a scalar of mass at 750 GeV).

3) Finite M_Θ effects on the QCD corrections. We will neglect these here.

Although the higher-order corrections to φ production are smaller than the ones to Higgs production in the SM, they are essential for allowing a signal as large as that indicated by the diphoton excess.

The s-channel production of φ is followed by the $\varphi \to AA'$ and $A \to \gamma\gamma$ decays (see Figure 1). The nonresonant contribution to $gg \to AA'$ due to the (2.17) interaction is two orders of magnitude smaller, and it can be safely ignored. The total cross section times branching fractions of the diphoton signal at the 13 TeV LHC is thus

$$\begin{aligned} \sigma_{\gamma\gamma} &\equiv \sigma(pp \to \varphi \to A'A \to A'\gamma\gamma) \\ &= K_{\mathrm{N^3LO}}\, \sigma_{\mathrm{LO}}(pp \to \varphi X)\, B(\varphi \to AA')\, B(A \to \gamma\gamma) \quad . \end{aligned} \tag{2.25}$$

For $M_\varphi = 780$ GeV, $M_\Theta = 800$ GeV, $M_A = 750$ GeV, $M_{A'} \ll M_\varphi - M_A$, and using the values for dimensionless couplings given in Eq. (2.19), we find $\sigma_{\gamma\gamma} \approx 6.7$ fb. For other values of M_φ and M_Θ, the signal cross section $\sigma_{\gamma\gamma}$ is shown in Figure 2. The CMS signal cross section is $3.7^{+1.5}_{-1.3}$ fb at $\sqrt{s} = 13$ TeV, based on the combination of the Run 2 and

Run 1 data sets [2]. The ATLAS signal cross section has been estimated in [26] to lie between approximately 5 fb and 12 fb in the case of a narrow resonance. Thus, the 2-step model presented here straightforwardly accommodates the measured signal rate.

The $\gamma\gamma$ signal rate can be large enough to explain the ATLAS peak only for $M_\Theta \lesssim 1.2$ TeV. The current lower limit on M_Θ can be derived from the CMS search in the final state with a pair of dijet resonances of equal mass [27]. The cross section for the process $pp \to \Theta\Theta$ depends on a single parameter, M_Θ, as the Θ interaction with gluons is fixed by QCD, and there is no $SU(2)_W$ invariant coupling of Θ to the SM quarks. The 1-loop process $\Theta \to gg$, which proceeds through the trilinear coupling λ_Θ, has a branching fraction near 100%. The CMS limit of about 1 pb on the cross section for pair production of dijets corresponds to $M_\Theta \gtrsim 400$ GeV (note that the theoretical prediction shown in Figure 7 of [27] refers to a spin-1 particle, whose production rate is almost 40 times larger than for the spin-0 color octet discussed here [28]).

In order to avoid A' decays into photons, we take the A' mass $M_{A'}$ sufficiently small so that the decay is outside the electromagnetic calorimeter. The decay length of a light A' is

$$L_{A'} \approx \frac{y_\psi^2 M_A^3}{y_\psi'^2 M_{A'}^3 \, \Gamma(A \to \gamma\gamma)} \quad , \tag{2.26}$$

where y'_ψ is related to m_ψ by Eq. (2.12). For example, if $M_{A'} < 80$ MeV and $y'_\psi = y_\psi$, then the A' decay length is longer than 12 m.

A lower limit on $M_{A'}$ is set by star cooling constraints. Values of $M_{A'}$ below about 6 MeV make the decay length comparable to the size of a supernova core, so A' emission may modify the supernova temperature [29]. Even for $M_{A'} < 6$ MeV though, the A' mean-free path may be smaller than the supernova core because an $A'A'gg$ interaction is induced at one loop by the potential term proportional to κ_2 in Eq. (2.7). In any case, the range of $M_{A'}$ consistent with all the constraints spans at least an order of magnitude. Thus, we can assume that $M_{A'} \ll M_\varphi - M_A$, and that the A' gives rise to missing transverse energy at the LHC. In Section 4 we will show that the kinematic distributions predicted in this 2-step model are in agreement with those presented by ATLAS [1].

The vectorlike lepton ψ is a weak singlet and has hypercharge +1 (*i.e.*, electric charge +1). Therefore, an $H\bar{L}_L\psi_R$ Yukawa coupling to the SM lepton doublets L is gauge invariant. This coupling leads to mixing of ψ with the SM charged leptons. As a result, the main decay modes of the new heavy fermion are $\psi \to W\nu, Z\tau, h^0\tau$. The lower limits on m_ψ set at colliders are loose, of order 100 GeV [30].

Searches for vectorlike leptons produced in pairs at the LHC will provide a test for this model. One should recognize though that there is some flexibility in choosing the particles running in the loops that lead to $A \to \gamma\gamma$. For example, if instead of a vectorlike lepton there is a charged scalar that couples to ϕ, then the diphoton signal would not changed. By contrast, the presence of the color-octet scalar Θ in the production loop is a more robust feature. Note that if instead of Θ there were a vectorlike quark responsible for φ production through gluon fusion, then it would be difficult to avoid the coupling of A to the vectorlike quark so that the main decay of A would be into gluons, rendering a too small rate for $A \to \gamma\gamma$. Thus, searches for pair production of Θ are a more generic test of this 2-step model.

3 A strange-production model

In this section, we construct a model in which the diphoton resonance arises as part of a cascade decay of a new gauge boson Z' produced predominantly via strange-quark fusion

$$pp \to Z' \to \bar{\nu}_s N \ , \quad N \to \nu_s \Phi \ , \quad \Phi \to \gamma\gamma \tag{3.1}$$

where Φ is a (pseudo)scalar with $M_\Phi \simeq 750$ GeV, N is a SM-singlet heavy Dirac fermion, and ν_s is a sterile neutrino. Unlike the gluon-initiated model of Section 2, this model relies on sea-quark production. The production process could potentially be distinguished using differential distributions. For instance, variation in QCD radiation between quarks and gluons could lead to discernible differences in $N_{\rm jet}$ distributions, as we will show in Section 4.

3.1 New fields and symmetries

We introduce a new gauge symmetry $U(1)_{sb}$ under which the only SM states that are charged are the right-handed s and b quarks, which carry opposite charge. The Z' couplings are flavor diagonal as long as the right-handed quark mass and gauge eigenstates coincide, and so are not subject to constraints from flavor processes, *e.g.*, B_s mixing. This charge assignment leads to a $U(1)_Y\,[U(1)_{sb}]^2$ anomaly, requiring the introduction of new fermions f, f' ("anomalons") that are vectorlike with respect to the SM gauge groups (and $SU(3)_c \times SU(2)_W$ singlets) but chiral under $U(1)_{sb}$. An implication of the anomalons charged under both $U(1)_Y$ and $U(1)_{sb}$ is the loop-induced decays of the new

field	$SU(3)_c$	$SU(2)_W$	$U(1)_Y$	$U(1)_{sb}$
s_R	3	1	$-1/3$	$+1$
b_R	3	1	$-1/3$	-1
f_R	1	1	$+1$	$+1$
f'_R	1	1	$+1$	-1
f_L, f'_L	1	1	$+1$	0
N_{+R}	1	1	0	$+1$
N_{-R}	1	1	0	-1
N_L	1	1	0	0
ϕ', ϕ	1	1	0	$+1$

Table 1: Fields charged under the $U(1)_{sb}$ gauge symmetry. The spin is 0 for ϕ' and ϕ, and 1/2 for the anomalons (f, f'), the N fields, and the s_R and b_R quarks.

(pseudo)scalars to two photons.[2] We include three Weyl fermions $N_{\pm R}, N_L$, which are SM singlets and permit the cascade decay of the Z'. The relevant matter content of the theory is given in Table 1.

Along with the new fermions, the theory contains two new scalars charged under $U(1)_{sb}$, ϕ' and ϕ. We assume to a first approximation (discussed later) that the scalar potential respects a $\mathbb{Z}_2$ symmetry under which $\phi \to -\phi$ and $\phi' \to \phi'$. Constraints on deviations from SM Higgs branching fractions, as well as the dihiggs production rate and $t\bar{t}$ resonance searches limit the size of couplings between the SM Higgs and ϕ and ϕ' so we also assume that the couplings to the SM Higgs field are small (we will discuss this more in Section 3.2).

Under these assumptions, the most general renormalizable potential for the new spin-0 fields is

$$V \supset -M_{\phi'}^2 \left|\phi'\right|^2 + M_\phi^2 \left|\phi\right|^2 + \frac{\lambda_{\phi'}}{4} \left|\phi'\right|^4 + \frac{\lambda_\phi}{4} \left|\phi\right|^4 + \lambda_{\phi'\phi} \left|\phi'\right|^2 \left|\phi\right|^2 + \left[\lambda'_{\phi'\phi} (\phi^\dagger \phi')^2 + \text{H.c.}\right] \quad . \tag{3.2}$$

We take the quartic couplings and the mass-squared parameters to be positive. In this

[2] A model with similar charge assignment was proposed in a completely different context in [31]. As an alternative model, the coupling of the Z' to the SM could be through a higher-dimension operator, generated by integrating out fermions transforming under the SM gauge group as the right-handed strange quark [32].

limit, a non-zero VEV develops for ϕ' while $\langle\phi\rangle = 0$. As such, ϕ' is responsible for spontaneously breaking $U(1)_{sb}$, giving mass to the Z' as well as to the anomalons. The additional scalar ϕ will be the diphoton resonance, as we discuss below. After $U(1)_{sb}$ breaking the real spin-0 fields are

$$\phi' = \langle\phi'\rangle + \frac{\varphi'}{\sqrt{2}} \qquad , \qquad \phi = \frac{1}{\sqrt{2}}\left(\varphi + iA\right). \tag{3.3}$$

The mass of the new gauge bosons $M_{Z'} = \sqrt{2} g_z \langle\phi'\rangle$, where g_z is the $U(1)_{sb}$ gauge coupling. We assume that $M_{\varphi'}$ is sufficiently large that this state does not play a role in the phenomenology of interest.

The scalars couple to anomalons via

$$\mathcal{L} \supset -y'_f \phi'^\dagger \bar{f}_L f_R - y'_{f'} \phi' \bar{f}'_L f'_R - y_f \phi^\dagger \bar{f}_L f_R - y_{f'} \phi \bar{f}'_L f'_R + \text{H.c.} \tag{3.4}$$

The anomalons acquire a mass from their coupling to ϕ', $m_{f^{(\prime)}} = y'_{f^{(\prime)}} \langle\phi'\rangle$, while the Yukawa couplings of ϕ permit the physical states φ and A to decay to photons at one loop. We impose $m_f, m_{f'} > M_{Z'}/2$ to forbid the decay of Z'_{sb} into anomalons. Additional Yukawa terms of the type $\phi'^\dagger \bar{f}'_L f_R$ or $\phi' \bar{f}_L f'_R$, or similarly with ϕ' replaced by ϕ, may be present, leading to $f - f'$ mixing; however, such mixing is not consequential in what follows.

The SM Yukawas for b and s quarks are forbidden by $U(1)_{sb}$ but are allowed at dimension 5 and can be generated from a renormalizable theory by integrating out vectorlike fermions that have the same quantum numbers as b_R. For order one couplings these heavy fermions must be lighter than $\langle\phi'\rangle / y_q^{SM} \sim 10 - 100$ TeV. There are additional renormalizable terms $\phi' \bar{f}^c_R \ell_R$ which mix the anomalons with the right-handed leptons and allow the anomalons to decay to $W\nu$, $Z\ell$.

The scalars also couple to the N fermions:

$$\mathcal{L} \supset -y'_+ \phi'^\dagger \bar{N}_L N_{+R} - y'_- \phi' \bar{N}_L N_{-R} - y_+ \phi^\dagger \bar{N}_L N_{+R} - y_- \phi \bar{N}_L N_{-R} + \text{H.c.} \tag{3.5}$$

We assume that the N-number violating mass terms of the form $\bar{N}_L N^c_L$ and $\bar{N}^c_{+R} N_{-R}$ are suppressed (or even completely forbidden) by a global $U(1)_N$ symmetry. As such, for $\langle\phi'\rangle \neq 0$, the couplings $y'_\pm$ give mass to a Dirac fermion N, whose left-handed component is N_L (see Table 1), and whose right-handed component is a linear combination of $N_{\pm R}$:

$$N_R = c_N N_{+R} + s_N N_{-R} \quad . \tag{3.6}$$

The orthogonal linear combination of $N_{\pm R}$ forms a massless 2-component fermion ν_s,

$$\nu_{sR} = -s_N N_{+R} + c_N N_{-R} \quad , \tag{3.7}$$

with the mixing given by

$$s_N, c_N = \frac{y'_{\mp}}{\sqrt{{y'_+}^2 + {y'_-}^2}} \quad . \tag{3.8}$$

As ν_s is a massless (or nearly massless if a small Majorana mass is introduced) fermion that is a SM singlet, it is appropriate to refer to it as a sterile neutrino. Higher-dimensional operators may induce some small mixing between ν_s and the SM neutrinos; we will ignore here these effects. The mass of N is related to the ϕ' VEV by

$$m_N = \frac{y'_-}{s_N} \langle \phi' \rangle \quad . \tag{3.9}$$

The Yukawa couplings of the components of ϕ to the physical fermions N and ν_s are

$$\mathcal{L} \supset -\frac{1}{\sqrt{2}} \Big[(-y_+ s_N + y_- c_N)\varphi + (y_+ s_N + y_- c_N) iA \Big] \bar{N}_L \nu_{sR} + \text{H.c.} \tag{3.10}$$

Note that any couplings of φ or A that can lead to their decays to $\nu_s \nu_s$ vanish in the limit of massless ν_s. The couplings of the Z' boson to the electrically-neutral fermions are given by

$$\mathcal{L}_{\text{kin}} \supset g_z (c_N^2 - s_N^2) \left(\bar{N}_R \not{Z}' N_R - \overline{\nu}_{sR} \not{Z}' \nu_{sR} \right) - 2 g_z c_N s_N \left(\bar{N}_R \not{Z}' \nu_{sR} + \text{H.c.} \right) \quad . \tag{3.11}$$

We now have the interactions necessary to describe the production and decay of the particles that lead to the diphoton signal, as shown in Figure 3.

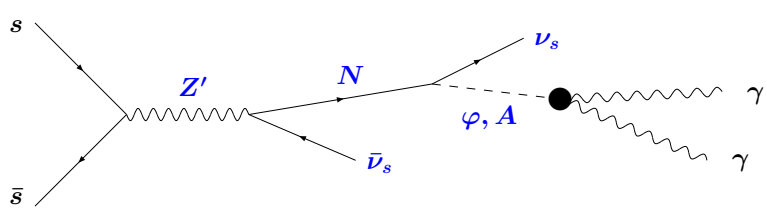

Figure 3: Diagram for φ/A production at the LHC in the 3-step Z'_{sb} model. The sterile neutrinos ν_s escape the detector.

3.2 Production and decay

The dominant partial width of the Z' is to pairs of right-handed s and b quarks,

$$\Gamma(Z' \to s\bar{s}) \simeq \Gamma(Z' \to b\bar{b}) \simeq \frac{g_z^2}{8\pi} M_{Z'} \quad , \tag{3.12}$$

while the widths to the neutral fermions are

$$\begin{aligned} \Gamma(Z' \to \nu_s \bar{\nu}_s) &= \frac{g_z^2 (c_N^2 - s_N^2)^2}{24\pi} M_{Z'} \quad , \\ \Gamma(Z' \to N\,\nu_s) &= \frac{g_z^2 s_N^2 c_N^2}{3\pi} M_{Z'} \left(1 - \frac{3m_N^2}{2M_{Z'}^2} + \frac{m_N^6}{2M_{Z'}^6}\right) \quad . \end{aligned} \tag{3.13}$$

In a compressed spectrum the second decay is phase-space suppressed, $\Gamma(Z' \to N\,\nu_s) \approx g_z^2 s_N^2 c_N^2 (M_{Z'} - m_N)^2/(\pi M_{Z'})$.

In turn, the 2-body decays of N are

$$\begin{aligned} \Gamma(N \to \varphi\,\nu_s) &= \frac{(-y_+ s_N + y_- c_N)^2}{64\pi}\, m_N \left(1 - \frac{M_\varphi^2}{m_N^2}\right)^2 \quad , \\ \Gamma(N \to A\,\nu_s) &= \frac{(y_+ s_N + y_- c_N)^2}{64\pi}\, m_N \left(1 - \frac{M_A^2}{m_N^2}\right)^2 \quad . \end{aligned} \tag{3.14}$$

These also become small as the splitting between N and the scalar in the final state becomes small. Thus, the 3-body decay to a pair of s or b quarks, through an off-shell Z', may compete. This width is

$$\Gamma(N \to \nu_s q\bar{q}) = \frac{3g_z^4\, s_N^2 c_N^2\, M_{Z'}^2}{16\pi^3 m_N} \left(1 - \frac{m_N^2}{2M_{Z'}^2} - \frac{m_N^4}{6M_{Z'}^4} - \left(1 - \frac{M_{Z'}^2}{m_N^2}\right) \ln\left(1 - \frac{m_N^2}{M_{Z'}^2}\right)\right) \quad , \tag{3.15}$$

where we have ignored the quark masses. The lack of significant missing energy observed in the signal events, see Section 4, requires somewhat small mass splittings $M_{Z'} \gtrsim m_N \gtrsim$ 750 GeV. As a result, N decays to the diphoton resonance are phase-space suppressed, while the 3-body decays to $\nu_s q\bar{q}$ are not. To compensate for this and achieve the observed diphoton rate the couplings $y_\pm$ cannot be too small. Furthermore, the phase-space suppression for $Z' \to N\nu_s$ means that there can be substantial contribution to $N\nu_s$ production from an off-shell Z'. This non-resonant production of the diphoton state can alter the kinematic distributions considerably, injecting additional missing transverse energy into the event relative to the case of on-shell production.

Note that this feature does not occur in the 2-step model, but rather is particular to the phase-space suppressed production of fermions via a vector boson. In the center-of-mass frame, the 3-step process is proportional to the final state velocity β_f^3, whereas near-threshold scalar production from a scalar resonance (as in the 2-step model) is proportional to β_f. As a result, gains from going off-shell are more substantial in the 3-step model, leading to a significant contribution from non-resonant Z' production.

So far, we have remained agnostic as to whether φ or A is the observed resonance, since both can decay to diphotons (as well as ZZ and γZ) through a loop of anomalons. Integrating out the anomalons leads to effective dimension-5 operators coupling the scalars to the hypercharge field strength,

$$\frac{\alpha}{6\sqrt{2}\pi\cos^2\theta_w}\left(\frac{y_f}{m_f}+\frac{y_{f'}}{m_{f'}}\right)\varphi B^{\mu\nu}B_{\mu\nu}+\frac{\alpha}{8\sqrt{2}\pi\cos^2\theta_w}\left(-\frac{y_f}{m_f}+\frac{y_{f'}}{m_{f'}}\right)A\,B^{\mu\nu}\tilde{B}_{\mu\nu}\ . \quad (3.16)$$

The resulting widths are

$$\Gamma(\varphi\to\gamma\gamma) = \frac{\alpha^2}{288\pi^3}\left(\frac{y_f}{m_f}+\frac{y_{f'}}{m_{f'}}\right)^2 M_\varphi^3\ , \quad (3.17)$$

$$\Gamma(A\to\gamma\gamma) = \frac{\alpha^2}{128\pi^3}\left(-\frac{y_f}{m_f}+\frac{y_{f'}}{m_{f'}}\right)^2 M_A^3\ . \quad (3.18)$$

As the anomalons are $SU(2)_W$ singlets, the A pseudoscalar exhibits characteristic branching fractions to diphotons $B(A\to\gamma\gamma)=59.5\%$, and so can serve as the resonance. Whether or not φ has the same branching fraction and also contributes to the diphoton rate depends on details of the model we have not yet discussed. Specifically, additional terms in the scalar potential can give rise to terms that mix φ and the SM Higgs boson.[3] For instance, a term

$$\Delta V=\lambda_{\phi\phi' H}\left(\phi^\dagger\phi'+\phi\phi'^\dagger\right)|H|^2 \quad (3.19)$$

will lead to $\varphi-h^0$ mixing, as well as inducing a VEV for ϕ. Note that this term violates the $\mathbb{Z}_2$ symmetry $\phi\to-\phi$, but this parity is also collectively broken by the Yukawas, so it cannot be used to set the above term to zero. The explicit breaking by the Yukawa couplings to the anomalons leads to this term being generated at two loops, so it is consistent to treat ΔV as a small perturbation on the potential of (3.2).[4]

Thus, one can imagine two scenarios. In the first case, the $\varphi-h^0$ mixing is very suppressed, $\lambda_{\phi\phi' H}\lesssim 10^{-4}$, such that φ decays predominantly via anomalon loops. Then,

[3]Terms mixing φ' and h^0 may also be present, but are irrelevant for the diphoton signal. Such terms must simply be small enough to be consistent with measurements of Higgs couplings.

[4]Similar reasoning motivates neglecting the mass-mixing term $b^2\phi^\dagger\phi'$, which only arises at one loop.

both A and φ can contribute to the diphoton rate. A mass splitting between φ and A could broaden the diphoton signal, potentially explaining the preference for a wide resonance preferred by the ATLAS data. This splitting can be generated from ΔV, $\lambda'_{\phi'\phi}$ and the mass-mixing term.

Alternatively, $\varphi - h^0$ mixing may be non-negligible, leading to additional decays of φ to SM states, notably $\varphi \to t\bar{t}$. As such, the diphoton signal comes entirely from A and the model predicts a second resonance of mass close to 750 GeV with branching fractions characteristic of a singlet mixing with the Higgs. Since φ no longer contributes to the diphoton rate, the decay $N \to A\,\nu_s$ must dominate over $N \to \varphi\,\nu_s$, for instance due to $M_\varphi > m_N$ or coincidental cancellations as for $y_+ \simeq y_-$ (supposing $c_N \simeq s_N$).

We now present a viable example parameter point:

$$\begin{aligned} &M_{Z'} = 790 \ \text{GeV} \ , \quad g_z = 0.5 \Rightarrow \langle\phi'\rangle \approx 1.1 \ \text{TeV} \ , \\ &m_N = 760 \ \text{GeV} \ , \quad y'_+ = 0.45 \Rightarrow y'_- \approx 0.51 \ , \\ &m_f = m_{f'} = 500 \ \text{GeV} \Rightarrow y'_f = y'_{f'} \approx 0.45 \ . \end{aligned} \tag{3.20}$$

The choice of $y'_\pm$ is chosen to give large N mixing. At this point the Z' width and relevant branching fraction are $\Gamma_{Z'} \approx 16$ GeV, $B(Z' \to N\,\nu_s) \approx 2.7 \times 10^{-3}$. However, since the phase space for the decay $Z' \to N\,\nu_s$ is limited, approximately 30% of $\sigma(pp \to N\,\nu_s)$ comes from off-resonance production. Including a K-factor[5] of $K_{\rm NLO} = 1.3$ and using MadGraph [22] to calculate the leading order production cross section we find

$$\sigma^{\rm NLO}_{\rm 13TeV}(pp \to N\,\nu_s) \simeq 19 \ \text{fb} \ . \tag{3.21}$$

The width for the 3-body decay of N is $\Gamma(N \to \nu_s jj) \approx 14$ MeV and the values of $y_\pm$ must be large enough that the 2-body decay $N \to \nu_s\varphi/A$ dominates this small width. The required size will depend upon whether both φ and A contribute to the $\gamma\gamma$ signal or just A. In Figure 4, we show the signal rate for both possibilities

$$\sigma_{\gamma\gamma} = K_{\rm NLO}\,\sigma_{\rm LO}(pp \to N\,\nu_s)\,B(N \to \Phi\nu_s)\,B(\Phi \to \gamma\gamma) \ , \tag{3.22}$$

where Φ can represent only A or a combination of A and φ. From Figure 4 we see that if $y_- = y_+ \approx 0.9$ (1.5) the decay of the N is predominantly to A and $\sigma_{\gamma\gamma}$ is large enough to explain the lower value for the CMS (ATLAS) diphoton excess, see Figure 2. We show the corresponding kinematic distributions for this parameter point in Section 4.

[5]Due to different production channels, the NLO correction for a Z' produced from sea quarks could be up to twice as large as that for a sequential Z', $K_{\rm NLO} \approx 1.2$ [33]. We view our estimate as conservative.

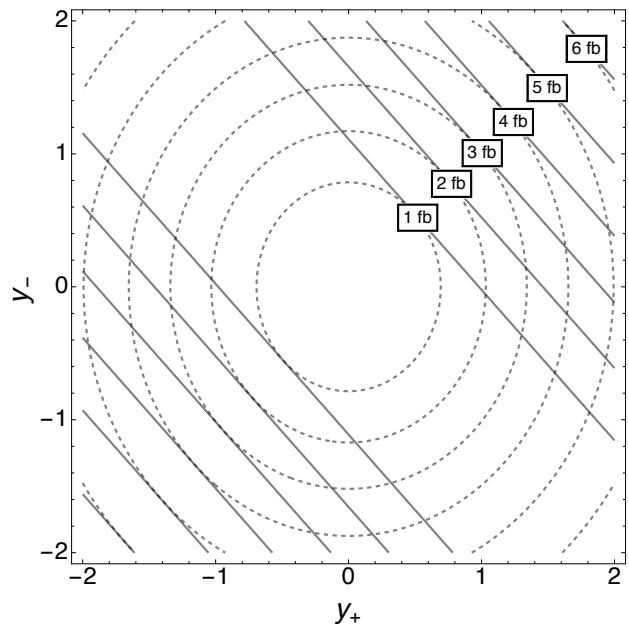

Figure 4: Contours of signal cross section $\sigma_{\gamma\gamma}$ as a function of the Yukawa couplings of ϕ to N, $y_\pm$ (see (3.5)), for the example parameter point (3.20) discussed in the text. Solid contours correspond to the case where only the pseudoscalar A contributes to the signal, whereas dashed contours include both decays $N \to \varphi\,\nu_s$, $A\,\nu_s$.

For this benchmark point the production cross section of Z' at the 8 TeV LHC is,

$$\sigma^{\rm NLO}_{8\rm TeV}(pp \to Z') \simeq 1 \text{ pb} \quad , \tag{3.23}$$

again including a K-factor of $K_{\rm NLO} = 1.3$. This is consistent with the current limits on dijet resonances [34].

4 Kinematic distributions

In this section, we compare the differential distributions for the models described in Sections 2 and 3 to those published by the ATLAS collaboration [1]. We also show distributions for the canonical interpretation of the signal in terms of resonant scalar produced through gluon fusion and decaying directly to two photons, $gg \to \varphi \to \gamma\gamma$. Due to limited statistics, the data cannot yet distinguish between these models, but can constrain their allowed parameter space. We highlight notable features that could potentially allow

discrimination in future—for a similar discussion of model discrimination[6] preceding the recent ATLAS publication, see [13]. In addition, we observe that kinematic distributions, particularly that for missing energy, can already place stringent constraints on certain models.

The various distributions are shown in Figure 5 and are generated as follows. Partonic events are generated in MadGraph [22], with showering carried out subsequent in PYTHIA 6.4 [36]. Detector simulation is carried out using DELPHES 3.3.0 [37]. For masses, we use the benchmark values given above, namely

$$M_\varphi = 780 \text{ GeV} \quad , \quad M_A = 750 \text{ GeV} \quad , \quad M_{A'} = 0 \tag{4.1}$$

for the 2-step model, and

$$M_{Z'} = 790 \text{ GeV} \quad , \quad m_N = 760 \text{ GeV} \quad , \quad M_A = 750 \text{ GeV} \quad , \quad m_{\nu_s} = 0 \tag{4.2}$$

for the 3-step model. For background, we take the distributions from SHERPA [38] given by ATLAS. While the distributions shown here are for unmatched samples, the distributions are not significantly altered by matching.

Total expected distributions for each model are obtained by combining a weighted amount of the signal distribution to the background distribution. In particular, based on the functional fit provided in [1], we take the expected number of background events in the window $m_{\gamma\gamma} \in [700, 840]$ GeV to be $N_b = 17$. We then add a signal corresponding to N_s events and renormalize the distributions. In other words, we take

$$\left(\frac{1}{N}\frac{dN}{dx}\right)_{\text{total}} = \frac{N_b}{N_s + N_b}\left(\frac{1}{N}\frac{dN}{dx}\right)_{\text{background}} + \frac{N_s}{N_s + N_b}\left(\frac{1}{N}\frac{dN}{dx}\right)_{\text{signal}} \tag{4.3}$$

where x represents a kinematic variable of interest. We consider a range of signal events $6 \leq N_s \leq 14$, and require events satisfy 700 GeV $\leq m_{\gamma\gamma} \leq$ 840 GeV and pass the ATLAS cuts. For simplicity, we take these to be $p_{T,\gamma_1} > 300$ GeV, $p_{T,\gamma_2} > 225$ GeV as for photons arising from a 750 GeV resonance, *i.e.*, with $m_{\gamma\gamma} \simeq 750$ GeV, but have confirmed that the given distributions are not particularly sensitive to this choice. The acceptance and cut efficiency for the various models is $\epsilon \simeq 0.6$; as such, for the luminosity $\mathcal{L} = 3.2$ fb^{-1}, this range of N_s corresponds to 3.1 fb $\leq \sigma_{\gamma\gamma} \leq$ 7.3 fb. The upper bound is chosen to reproduce the $N_o = 31$ total events observed by ATLAS in this window, whereas smaller cross sections represent a better fit to the combination of ATLAS and CMS datasets from both 8 TeV and 13 TeV [26].

[6] Kinematic distributions in a different model are discussed in, *e.g.*, [35].

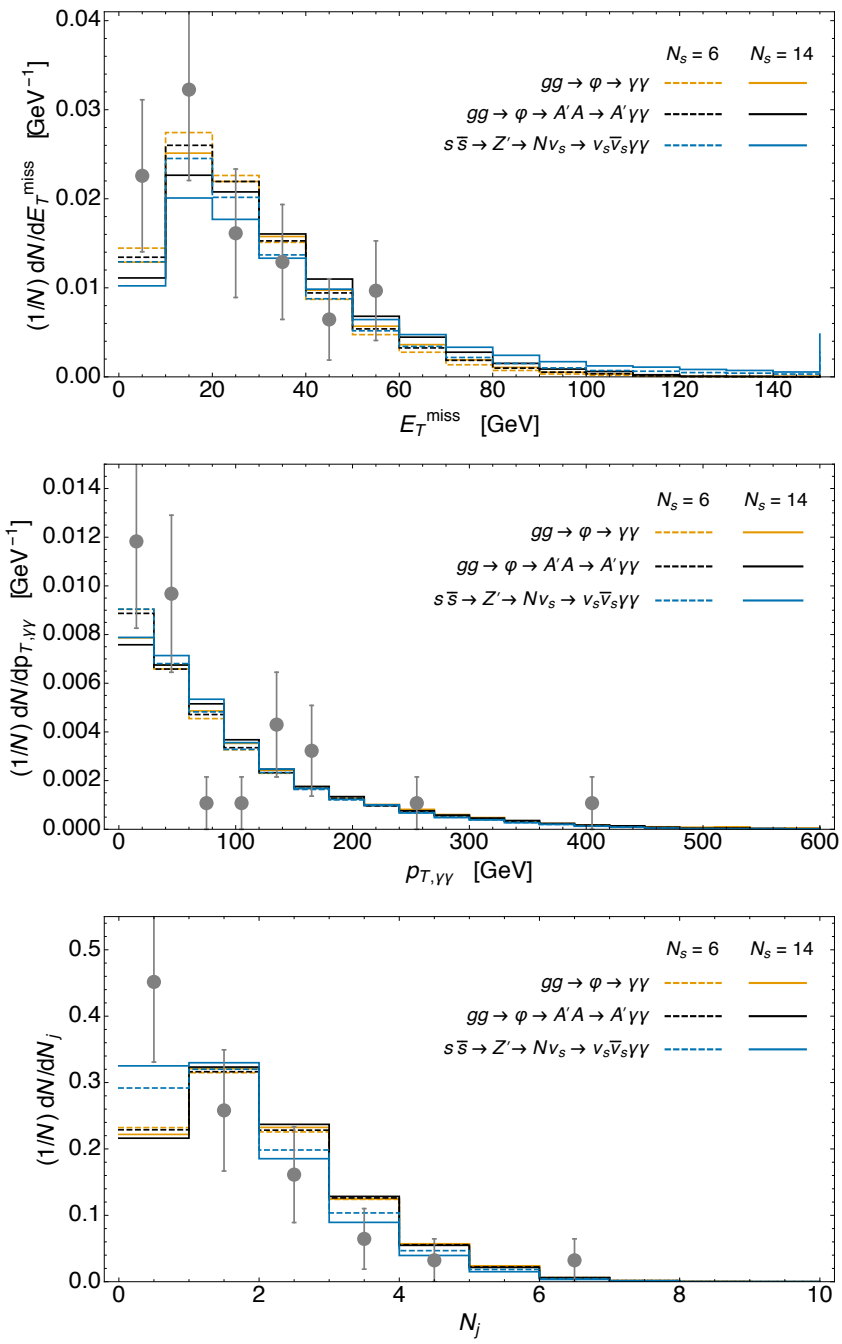

Figure 5: Normalized kinematic distributions for the 2-step, 3-step and canonical $gg \to \varphi \to \gamma\gamma$ models supposing $N_b = 17$ background events and $6 \leq N_s \leq 14$ signal events. The acceptance/cut efficiency is $\epsilon \simeq 0.6$, such that this choice corresponds to 3.1 fb $\leq \sigma_{\gamma\gamma} \leq$ 7.3 fb for 3.2 fb^{-1} of data. Data (gray dots) are taken from [1]. Top: Missing momentum; the uptick at the end corresponds to overflow, *i.e.*, events with $\not{E}_T > 150$ GeV. Middle: p_T of the $\gamma\gamma$ system. Bottom: Jet multiplicity; the overlap of the 2-step and canonical models (black and orange) is due to processes arising from the same initial state.

As the two models described above both feature additional particles that escape the detector, they exhibit somewhat longer tails in the missing transverse momentum ($\not{E}_T$) distributions compared to the simple $gg \to \varphi \to \gamma\gamma$ model. Correspondingly, increasing N_s shifts the distribution towards higher $\not{E}_T$ for these models, as can be seen in Figure 5. This is especially true for the 3-step model as two ν_s escape the detector, leading to additional $\not{E}_T$ and even an "overflow" of events with $\not{E}_T > 150$ GeV. By comparison, the $gg \to \varphi \to \gamma\gamma$ distribution does not change substantially.

Overall, the differential data are already sufficient to constrain models with significant missing energy. For instance, avoiding these constraints motivates the choice of somewhat small mass splittings used in the benchmark points. In fact, depending on the cross section $\sigma_{\gamma\gamma}$, even smaller splittings may be required for the 3-step model. For $N_s = 6$ (14), this model predicts 3.1 (6.6) events with $\not{E}_T > 60$ GeV, whereas ATLAS has observed 0. This corresponds to moderate (to severe) tension with the data, potentially requiring smaller splittings. However, there is also tension between a compressed spectrum and achieving sufficiently large branching fractions and rate. Moreover, as discussed in Section 3.2, off-shell Z' contributions will still yield events with non-negligible $\not{E}_T$. As such, the 3-step model may already be somewhat disfavored by current data. Though, we note that potential alternatives do exist for alleviating tension in the 3-step model, for instance if the ν_s state were to be somewhat massive and/or decay producing soft jets, perhaps in conjunction with another, lighter state that escaped the detector. For comparison, the expected number of events with $\not{E}_T > 60$ GeV is 1.3 (2.4) for the simple model and 1.7 (3.3) for the 2-step model, with background contributing 0.4 events.

Another notable difference between models appears in the N_j distribution, Figure 5. Specifically, gluon-initiated processes (the simple and 2-step models) both exhibit significantly higher jet multiplities than the sea quark ($s\bar{s}$ and $b\bar{b}$)-initiated 3-step model. While both types of process are consistent with current data, even this simple distribution may be useful in providing initial evidence for the production mechanism [39]. The $p_{T,\gamma\gamma}$ distributions, meanwhile, appear largely similar and currently consistent with data, and do not change significantly with N_s except at very low $p_{T,\gamma\gamma}$. This likely results from the small splittings required to satisfy the lack of observed $\not{E}_T$, which produce smaller boosts for the state that ultimately decays to two photons.

5 Conclusions

The possibility that a new, heavy particle decaying to two photons has been observed at ATLAS and CMS raises pressing questions: What might the production mechanism be? Is this particle produced alone, or in association with other states? Is it wider than the experimental resolution, or perhaps the resonance is made up of multiple narrow states nearby in mass? More data may even help distinguish whether the 750 GeV state decays to two photons as opposed to two pairs of highly-collimated photons resulting from the decay of a light intermediate state [40].

In this paper, we have proposed two weakly-coupled models capable of explaining the observed excess. Both feature additional final state particles, resulting in missing transverse momentum that could potentially be used to distinguish these models from the minimal interpretation in which the 750 GeV scalar is directly produced in gluon fusion. We have emphasized that even the limited kinematic information presented by the experiments thus far [1] already restricts the parameter ranges. Furthermore, the additional structure present in these models could be revealed by looking at other kinematic distributions such as M_T. In addition, these models provide viable examples of different initial states: gluons in the 2-step model (Section 2) and sea quarks in the 3-step model (Section 3). Differences in initial state radiation from quarks and gluons may appear in, *e.g.*, jet multiplicity distributions.

A distinctive feature of our models is that the particle produced in the s-channel is different from the one that decays to $\gamma\gamma$. This avoids the tension between simultaneously achieving a sufficiently large production via gluon fusion and a sufficiently large diphoton branching fraction (overcoming the decay back to jets), which requires the particles running in the loops to have large charges or multiplicities (see, *e.g.*, [12]).

In the 2-step model, the particle produced in the s-channel (φ) and the particle that decays into photons (A) are the two components of a complex scalar field whose VEV is much smaller than its mass. Consequently, their masses are naturally almost degenerate, leading to little activity in the event besides the two high-p_T photons.

In the 3-step model, a spin-1 particle (Z') is produced in the s-channel, and two spin-0 particles (A and φ) decay into $\gamma\gamma$. One notable feature of this model is that the process responsible for generating the signal does not involve loops of colored particles; production occurs at tree level, while the diphoton decay occurs via loops of "anomalons" required by the consistency of the theory. Although all their masses are set by the VEV that

breaks the gauged $U(1)$ symmetry, a mass splitting between the Z' and the scalars of less than 10%, as indicated by the kinematic distributions, requires some tuning. While it could simply be a coincidence, there are some possible explanations for this small mass splitting. For example, in models where multiple particles have masses proportional to a single scale of spontaneous symmetry breaking, mass relations could be the result of renormalization group fixed ratios as in, *e.g.*, [41]. A small mass splitting between A and φ is natural, and may account for the wider resonance suggested by the ATLAS fit.

We also observe that, depending on the spins of the particles involved, off-shell contributions to the diphoton rate can be significant in certain models because of relatively small splittings. It is important to take these effects into account as they can significantly alter kinematic distributions relative to the case where all intermediate-state particle are on-shell.

More broadly, it is interesting to consider the potential implications of the diphoton resonance for physics beyond the Standard Model. For instance, if the signal is due to a scalar field exhibiting relatively large $\mathcal{O}(1)$ Yukawa coupling to new fermions, we may be confronted with a second hierarchy problem and a new challenge as to whether naturalness is a good guiding principle. Should the putative signal be confirmed, it will undoubtedly provide important insight into physics beyond the Standard Model.

Acknowledgments: BD and PJF would like to thank University of Oregon, and the organizers of the workshop "Emerging New Physics at the LHC," for hospitality during the very final stages of this work. This work was supported by the DoE under contract number de-sc0007859 and Fermilab, operated by Fermi Research Alliance, LLC under contract number DE-AC02-07CH11359 with the United States Department of Energy.

References

[1] ATLAS collaboration, "Search for resonances in diphoton events with the ATLAS detector at $\sqrt{s} = 13$ TeV," ATLAS-CONF-2016-018.

[2] CMS Collaboration, "Search for new physics in high mass diphoton events in 3.3 fb^{-1} of proton-proton collisions at $\sqrt{s} = 13$ TeV and combined interpretation of searches at 8 TeV and 13 TeV," note PAS-EXO-16-018, March 2016.

[3] ATLAS collaboration, "Search for resonances decaying to photon pairs in 3.2 fb^{-1} of pp collisions at $\sqrt{s} = 13$ TeV," note CONF-2015-081, December 2015.

[4] CMS Collaboration, "Search for new physics in high mass diphoton events in proton-proton collisions at 13TeV," note PAS-EXO-15-004, December 2015

[5] V. Khachatryan *et al.* [CMS Collaboration], "Search for diphoton resonances in the mass range from 150 to 850 GeV in pp collisions at $\sqrt{s} = 8$ TeV," Phys. Lett. B **750**, 494 (2015) [arXiv:1506.02301 [hep-ex]].

[6] F. Staub *et al.*, "Precision tools and models to narrow in on the 750 GeV diphoton resonance," arXiv:1602.05581 [hep-ph].

[7] R. Franceschini, G. F. Giudice, J. F. Kamenik, M. McCullough, F. Riva, A. Strumia and R. Torre, "Digamma, what next?," arXiv:1604.06446 [hep-ph].

[8] P. J. Fox, D. Tucker-Smith and N. Weiner, "Higgs friends and counterfeits at hadron colliders," JHEP **1106**, 127 (2011) doi:10.1007/JHEP06(2011)127 [arXiv:1104.5450 [hep-ph]].

[9] W. S. Cho, D. Kim, K. Kong, S. H. Lim, K. T. Matchev, J. C. Park and M. Park, "750 GeV diphoton excess may not imply a 750 GeV resonance," Phys. Rev. Lett. **116**, no. 15, 151805 (2016) [arXiv:1512.06824 [hep-ph]].

[10] F. P. Huang, C. S. Li, Z. L. Liu and Y. Wang, "750 GeV Diphoton Excess from Cascade Decay," arXiv:1512.06732 [hep-ph].

[11] W. Altmannshofer, J. Galloway, S. Gori, A. L. Kagan, A. Martin and J. Zupan, "750 GeV diphoton excess," Phys. Rev. D **93**, no. 9, 095015 (2016) [arXiv:1512.07616].

[12] R. Franceschini *et al.*, "What is the $\gamma\gamma$ resonance at 750 GeV?," JHEP **1603**, 144 (2016) [arXiv:1512.04933 [hep-ph]].

[13] J. Bernon, A. Goudelis, S. Kraml, K. Mawatari and D. Sengupta, "Characterising the 750 GeV diphoton excess," arXiv:1603.03421 [hep-ph].

[14] M. Badziak, M. Olechowski, S. Pokorski and K. Sakurai, "Interpreting 750 GeV diphoton excess in plain NMSSM," arXiv:1603.02203 [hep-ph].

[15] R. Boughezal and F. Petriello, "Color-octet scalar effects on Higgs boson production in gluon fusion," Phys. Rev. D **81**, 114033 (2010) [arXiv:1003.2046 [hep-ph]].

[16] B. A. Dobrescu, G. D. Kribs and A. Martin, "Higgs Underproduction at the LHC," Phys. Rev. D **85**, 074031 (2012) [arXiv:1112.2208 [hep-ph]].
K. Kumar, R. Vega-Morales and F. Yu, "Effects from New Colored States and the Higgs Portal on Gluon Fusion and Higgs Decays," Phys. Rev. D **86**, 113002 (2012) Erratum: [Phys. Rev. D **87**, no. 11, 119903 (2013)] [arXiv:1205.4244 [hep-ph]].

[17] Y. Bai and B. A. Dobrescu, "Heavy octets and Tevatron signals with three or four b jets," JHEP **1107**, 100 (2011) [arXiv:1012.5814 [hep-ph]].

[18] For a review, see A. Djouadi, "The Anatomy of electro-weak symmetry breaking. I: The Higgs boson in the standard model," Phys. Rept. **457**, 1 (2008) [hep-ph/0503172].

[19] M. Steinhauser, "Higgs decay into gluons up to $O(\alpha_s^3 G_F m_t^2)$," Phys. Rev. D **59**, 054005 (1999) [hep-ph/9809507].

[20] K. A. Olive *et al.* [Particle Data Group Collaboration], "Review of Particle Physics," Chin. Phys. C **38**, 090001 (2014).

[21] A. Alloul, N. D. Christensen, C. Degrande, C. Duhr and B. Fuks, "FeynRules 2.0 - A complete toolbox for tree-level phenomenology," Comput. Phys. Commun. **185**, 2250 (2014) [arXiv:1310.1921].

[22] J. Alwall, R. Frederix, S. Frixione, V. Hirschi, F. Maltoni, O. Mattelaer, H.-S. Shao, T. Stelzer, P. Torrielli, M. Zaro, "The automated computation of tree-level and NLO differential cross sections, and their matching to parton shower simulations," JHEP **1407**, 079 (2014) [arXiv:1405.0301].

[23] J. M. Campbell, R. K. Ellis and W. T. Giele, "A Multi-Threaded Version of MCFM," Eur. Phys. J. C **75**, no. 6, 246 (2015) [arXiv:1503.06182 [physics.comp-ph]].

[24] C. Anastasiou, C. Duhr, F. Dulat, E. Furlan, T. Gehrmann, F. Herzog, A. Lazopoulos and B. Mistlberger, "High precision determination of the gluon fusion Higgs boson cross-section at the LHC," arXiv:1602.00695 [hep-ph].

[25] C. Anastasiou, C. Duhr, F. Dulat, E. Furlan, T. Gehrmann, F. Herzog, A. Lazopoulos and B. Mistlberger, "CP-even scalar boson production via gluon fusion at the LHC," arXiv:1605.05761 [hep-ph].

[26] M. R. Buckley, "Wide or Narrow? The Phenomenology of 750 GeV Diphotons," arXiv:1601.04751 [hep-ph].

[27] V. Khachatryan *et al.* [CMS Collaboration], "Search for pair-produced resonances decaying to jet pairs in proton-proton collisions at $\sqrt{s} = 8$ TeV," Phys. Lett. B **747**, 98 (2015) [arXiv:1412.7706 [hep-ex]].

[28] B. A. Dobrescu, K. Kong and R. Mahbubani, "Massive color-octet bosons and pairs of resonances at hadron colliders," Phys. Lett. B **670**, 119 (2008) [arXiv:0709.2378]. R. S. Chivukula, M. Golden and E. H. Simmons, "Multi - jet physics at hadron colliders," Nucl. Phys. B **363**, 83 (1991).

[29] G. G. Raffelt, "Stars as laboratories for fundamental physics : The astrophysics of neutrinos, axions, and other weakly interacting particles," University of Chicago Press (1996) 664 p.

[30] A. Falkowski, D. M. Straub and A. Vicente, "Vector-like leptons: Higgs decays and collider phenomenology," JHEP **1405**, 092 (2014) [arXiv:1312.5329 [hep-ph]].

[31] B. A. Dobrescu and C. Frugiuele, "Hidden GeV-scale interactions of quarks," Phys. Rev. Lett. **113**, 061801 (2014) [arXiv:1404.3947 [hep-ph]].

[32] P. J. Fox, J. Liu, D. Tucker-Smith and N. Weiner, "An Effective Z'," Phys. Rev. D **84**, 115006 (2011) [arXiv:1104.4127 [hep-ph]].

[33] G. Aad *et al.* [ATLAS Collaboration], "Search for high-mass dilepton resonances in pp collisions at $\sqrt{s} = 8$TeV," Phys. Rev. D **90**, no. 5, 052005 (2014) [arXiv:1405.4123].

[34] V. Khachatryan *et al.* [CMS Collaboration], "Search for narrow resonances in dijet final states at $\sqrt{s} = 8$ TeV with the novel CMS technique of data scouting," arXiv:1604.08907 [hep-ex].

[35] J. H. Collins, C. Csaki, J. A. Dror and S. Lombardo, "Novel kinematics from a custodially protected diphoton resonance," arXiv:1603.09350 [hep-ph].

[36] T. Sjostrand, S. Mrenna and P. Z. Skands, "PYTHIA 6.4 Physics and Manual," JHEP **0605**, 026 (2006) [hep-ph/0603175].

[37] J. de Favereau *et al.* [DELPHES 3 Collaboration], "DELPHES 3, A modular framework for fast simulation of a generic collider experiment," JHEP **1402**, 057 (2014) [arXiv:1307.6346 [hep-ex]].

[38] T. Gleisberg, S. Hoeche, F. Krauss, M. Schonherr, S. Schumann, F. Siegert and J. Winter, "Event generation with SHERPA 1.1," JHEP **0902**, 007 (2009) [arXiv:0811.4622 [hep-ph]].

[39] M. A. Ebert, S. Liebler, I. Moult, I. W. Stewart, F. J. Tackmann, K. Tackmann and L. Zeune, "Exploiting jet binning to identify the initial state of high-mass resonances," arXiv:1605.06114 [hep-ph].

[40] B. A. Dobrescu, G. L. Landsberg and K. T. Matchev, "Higgs boson decays to CP odd scalars at the Tevatron and beyond," Phys. Rev. D **63**, 075003 (2001) [hep-ph/0005308]. S. Chang, P. J. Fox and N. Weiner, "Visible Cascade Higgs Decays to Four Photons at Hadron Colliders," Phys. Rev. Lett. **98**, 111802 (2007) [hep-ph/0608310]. N. Toro and I. Yavin, "Multiphotons and photon jets from new heavy vector bosons," Phys. Rev. D **86**, 055005 (2012) [arXiv:1202.6377]. P. Draper and D. McKeen, "Diphotons from Tetraphotons in the decay of a 125 GeV Higgs at the LHC," Phys. Rev. D **85**, 115023 (2012) [arXiv:1204.1061]. S. D. Ellis, T. S. Roy and J. Scholtz, "Jets and photons," Phys. Rev. Lett. **110**, 122003 (2013) [arXiv:1210.1855]. S. Knapen, T. Melia, M. Papucci and K. Zurek, "Rays of light from the LHC," Phys. Rev. D **93**, 075020 (2016) [arXiv:1512.04928]. P. Agrawal, J. Fan, B. Heidenreich, M. Reece and M. Strassler, "Experimental considerations motivated by the diphoton excess at the LHC," arXiv:1512.05775. L. Aparicio, A. Azatov, E. Hardy and A. Romanino, "Diphotons from Diaxions," JHEP **1605**, 077 (2016) [arXiv:1602.00949]. U. Ellwanger and C. Hugonie, "A 750 GeV diphoton signal from a very light pseudoscalar in the NMSSM," JHEP **1605**, 114 (2016) [arXiv:1602.03344]. B. Dasgupta, J. Kopp and P. Schwaller, "Photons, photon jets and dark photons at 750 GeV and beyond," arXiv:1602.04692. P. Baratella, J. Elias-Miro, J. Penedo and A. Romanino, "A closer look to the sgoldstino interpretation of the diphoton excess," arXiv:1603.05682.

[41] J. Kearney and A. Pierce, "Dark sector mass relations from renormalization group focusing," Phys. Rev. D **88**, 095009 (2013) Erratum: [Phys. Rev. D **88**, 119902 (2013)] [arXiv:1309.4447 [hep-ph]].